CFD Letters

Journal homepage:
https://semarakilmu.com.my/journals/index.php/CFD_Letters/index
ISSN: 2180-1363

Control of Base Flows using Cavities at Supersonic Mach Number

Nik Deanna Asheera Nik Hishamuddin[1], Mir Sohail Ali[2], Ambareen Khan[3], Sher Afghan Khan[1,*], Khizar Ahmed Pathan[4], Ramchandra P. Chopade[4]

[1] Department of Mechanical and Aerospace Engineering, Faculty of Engineering, International Islamic University Malaysia, 53100 Kuala Lumpur, Malaysia
[2] Department of Civil Engineering, CSMSS Chh. Shahu College of Engineering, Aurangabad 431011, Maharashtra, India
[3] Centre for Instructional Technology and Multimedia, Universiti Sains Malaysia, 11700 Gelugor, Pulau Pinang, Malaysia
[4] Department of Mechanical Engineering, CSMSS Chh. Shahu College of Engineering, Aurangabad 431011, Maharashtra, India

ARTICLE INFO

Article history:
Received 7 April 2025
Received in revised form 12 May 2025
Accepted 8 June 2025
Available online 15 July 2025

Keywords:
Base pressure; cavity; CFD; passive control; L/D ratio

ABSTRACT

The occurrence of sudden expansion and flow at the blunt base in the aerospace industry is widespread. Due to flow separation at the base region, a recirculatory region forms, where the pressure is lower than the ambient pressure, resulting in a considerable base drag value. This study investigates the regulation of base flows that are suddenly expanded at a Mach number of 1.6. This study uses internal flow methods to simulate the flow field in the recirculation zone using the passive control technique in the form of a cavity. This paper covers geometrical parameters, including an area ratio of 2.25 and a length-to-diameter ratio of 1:6. Cavities were used as passive controls, and aspect ratios of 3:3 and 6:3 were used to control the base pressure. The location of the cavities was changed from 0.5D to 2D. The inertia parameters considered are the nozzle pressure ratio and the Mach number M = 1.6. The cavity is a passive control method to regulate base pressure and drag. Based on the results, improvements can be made to the aerodynamic design to meet the design specifications. This work also provides the design process for a passive control in terms of the cavity for suddenly expanded flow in a nozzle with a supersonic flow Mach number. The cavity does not adversely influence the flow field in the duct.

1. Introduction

This research paper delves into passive control strategies for managing base pressure in supersonic conditions, specifically at Mach 1.6. As propulsion systems, missiles and aircraft continuously strive for enhanced efficiency and reduced drag to optimize aerodynamic performance in high-speed flows, understanding and manipulating base pressure becomes pivotal. A significant challenge in aerodynamic vehicles is reducing drag, particularly when the Mach Number exceeds one. Increasing the surface area amplifies velocity, while decreasing the surface area reduces velocity. In divergent ducts, velocity increases; in convergent ducts, it decreases, opposite to subsonic flow behaviour.

[*] *Corresponding author.*
E-mail address: sakhan@iium.edu.my (Sher Afghan Khan)

https://doi.org/10.37934/cfdl.18.2.103123

The sudden growth of an axisymmetric flow field is a complex phenomenon characterized by the flow's separation, recirculation, and reattachment. A shear layer can partition a flow field into two primary regions: the flow recirculation zone and the primary flow region. The location where the dividing streamline makes contact with the wall is referred to as the reattachment line. Extensive data regarding sudden expansion problems can be found in the literature. Nevertheless, they are designed for certain instances involving flow and geometrical characteristics. The chapter will expand significantly if the entire literature is thoroughly reviewed. Hence, only the relevant articles to the current study will be examined in this context.

The base pressure control in suddenly expanded flows has been extensively studied due to its direct impact on base drag reduction, constituting a significant portion of the total aerodynamic resistance in high-speed aerospace applications. Flow control strategies are broadly classified into active and passive techniques. Active control methods, such as microjets, have effectively enhanced base pressure by altering the flow field near the recirculation zone; however, they require external energy input, which complicates their implementation in real-world aerospace systems where energy efficiency is a priority [1]. While active control techniques enable on-demand flow regulation, their dependence on external energy renders them less practical for many aerospace applications. In contrast, passive control mechanisms such as splitter plates and ribs modify the aerodynamic flow without requiring additional energy, making them more viable for practical use. Rathakrishnan [2] demonstrated that splitter plates reduce base drag by changing the recirculation zone. Still, their effectiveness depends on placement and aspect ratio, which may not always be adaptable to various aerodynamic configurations.

Rathakrishnan [3,4] researched the use of ribs as passive control devices in suddenly expanded flows, demonstrating that these structures generate secondary vortices that interact with the primary flow, thereby enhancing base pressure and reducing drag. These studies form the foundational work on rib-based passive control, but they primarily consider simple rib geometries without examining the influence of corrugation. The present study builds upon these findings by introducing corrugated ribs, which further manipulate the flow structure and improve pressure recovery. Vijayaraja *et al.,* [5] highlighted the significance of rib geometry in determining the effectiveness of passive flow control, while Sethuraman *et al.,* [6,7] emphasized the role of rib height and placement in minimizing the recirculation zone. Although these studies provided valuable insights, they did not explore how different rib geometries affect flow oscillations and shock-boundary layer interactions. The present study extends this research by systematically analyzing how corrugated ribs influence base pressure fluctuations, offering a more comprehensive understanding of their aerodynamic impact.

Despite previous research on passive control methods, certain limitations remain unaddressed. Khan *et al.,* [8–12] discussed various rib designs but did not quantify their effects on vortex shedding, shock standoff distance, or transient pressure fluctuations. These gaps are addressed in the current study, which conducts a detailed computational and experimental analysis of the role of corrugated ribs in regulating base pressure. CFD method has proven to be an essential tool in studying base pressure control mechanisms [10,11]. Ambareen *et al.,* [12,13] utilized the k-epsilon turbulence model to analyze the consequence of ribs on base pressure, confirming that CFD simulations can accurately capture the flow dynamics in suddenly expanded flows. However, their study did not focus on corrugated ribs or validate the numerical results with experimental data.

The impact of rib geometry on base pressure has also been explored through the finite volume method (FVM), as demonstrated by Ambareen *et al.,* [14]. While this study established the capability of FVM in simulating complex flow patterns, it did not investigate the aerodynamic trade-offs associated with different rib configurations. The present research provides an intense analysis by comparing multiple rib geometries and evaluating their effects on pressure recovery, turbulence intensity, and overall aerodynamic efficiency. Beyond rib-based passive control, studies on forward-facing cavities have shown their potential to reduce drag and mitigate aerodynamic heating [15]. Heubner and Utreja [16] investigated the influence of forward-facing cavities in hypersonic flow, demonstrating that they alter shock structures and reduce aerodynamic heating. While their findings contribute to the broader field of flow control, they did not consider passive rib configurations, which could offer similar benefits without compromising structural integrity.

Lorite *et al.,* [17] explored optimized rear cavity designs for drag reduction, revealing that cavity geometry is crucial in minimizing aerodynamic resistance. Sanmiguel [18] investigated the drag reduction produced by combining multi-cavity at the recirculation zone of a bluff body. However, their study focused on blunt-based bodies rather than forward-facing geometries or ribs, which are more relevant to the present investigation. Their findings suggest that optimizing geometric features can yield significant aerodynamic benefits, aligning with the study's objective to refine rib design for superior performance in suddenly expanded flows. Further studies by Kavimandan *et al.,* [19] and Saravanan *et al.,* [20] investigated the aerothermodynamic effects of forward-facing cavities, highlighting their potential to reduce thermal loads in high-speed aerospace applications. While their research aligns with the broader goal of enhancing aerodynamic performance, it does not directly address passive rib-based control methods.

Beyond the extensively studied passive control techniques, other innovative approaches have also been explored recently. Sudarshan [21] investigated the cavity's effect in the flow direction through a competing high-pressure jet combination at a Mach M = 6. Mohandas *et al.,* [22] investigated wave drag reduction on blunt bodies utilizing spikes with diverse apex geometries, demonstrating that spikes effectively alter shock formation and reduce aerodynamic drag. However, their study primarily focused on external flow aerodynamics, whereas the present research examines internal flow modification through the use of corrugated ribs. Engblom *et al.,* [23] conducted numerical studies and tests on forward-facing cavity flows at Mach numbers M> 5, providing insights into the complex flow behavior at extreme Mach numbers. While their study provided foundational knowledge on cavity-induced pressure regulation, it did not explore passive control methods, such as ribs, which can be integrated into similar aerodynamic designs.

Huang *et al.,* [24] conducted a parametric investigation into the reduction of heat flux and base drag using forward-facing cavities on blunt bodies. Their findings emphasized that cavity geometry is crucial in controlling aerodynamic heating and pressure fluctuations. This aligns with the present study's objective of optimizing geometric configurations for drag reduction. However, while their research examined cavity-induced drag reduction, the current study investigates the impact of rib configurations on base pressure control, addressing a gap in the literature by exploring how rib-induced vortices influence the recirculation region. Finally, Santos [25] analyzed the aerothermodynamics of rounded leading edges in hypersonic flow, accounting for real gas effects, with a focus on heat transfer and aerodynamic behavior under extreme conditions. While his work is crucial for understanding shockwave behavior and surface heating, it did not specifically address passive flow control mechanisms for drag reduction.

Khan *et al.,* [26,27] studied the effect of the base cavity and dimple cavities on the base flows at low Mach numbers. Sajli *et al.,* [28] numerically investigated the flow field of a non-circular cylinder at low speeds. Khan *et al.,* [29-30] studied the effect of expansion level, as well as the favorable pressure gradient, in a suddenly expanded flow at supersonic speeds using microjets. Results show that the control in the form of tiny jets is effective when the nozzles are under-expanded. These results reiterate that whether active or passive control methods become effective depends on the nozzles flowing under the influence of a favorable pressure gradient. Pandey *et al.,* [31] studied the effect of cavities at Mach 1.74 and used two cavities with aspect ratios of 1 and 2. Results indicate that the cavities are effective when the flow after exiting the nozzle falls within the cavity; otherwise, they are not effective. Hence, one must find the optimum location of the cavity to become effective, which increases the base pressure.

However, while the review highlights the potential of flow control techniques, it does not extensively focus on the role of ribs, particularly corrugated ribs, in mitigating base drag. This limitation highlights the need for the present study, which systematically examines the impact of corrugated ribs on base pressure enhancement at Mach unity.

The current research introduces several novel aspects of base pressure regulation. Firstly, employing corrugated ribs as a passive control mechanism remains an underexplored area, with limited studies available in the literature. This work systematically investigates the impact of rib height and placement on base pressure, providing valuable insights into the optimal design of corrugated ribs for enhancing base pressure. Secondly, this study employs advanced computational fluid dynamics (CFD) techniques, including the k-epsilon model, to account for turbulence and the finite volume method (FVM) to simulate the complex flow dynamics associated with corrugated ribs. The validation of CFD results against experimental data further enhances the credibility of this research. Lastly, the study highlights the potential environmental and energy implications of base pressure control, demonstrating that corrugated ribs could contribute to the development of more energy-efficient aerospace vehicles. By addressing the shortcomings of previous studies, the present research offers significant advancements in passive control techniques for supersonic and hypersonic flow applications.

The reviewed literature shows that significant research has been undertaken on passive and active control techniques for suddenly expanded flows. However, notable gaps remain. Most existing studies are concentrated on sonic and supersonic Mach numbers, while research on flow control at lower Mach numbers—ranging from subsonic to transonic—remains limited. Furthermore, the optimization of cavity geometry and placement has not been thoroughly explored. In this paper, we investigate passive control methods designed to influence base pressure at Mach 1.6, shedding light on their effectiveness in mitigating base pressure and, ultimately, base drag while optimizing the aerodynamic characteristics of high-speed vehicles.

2. CFD Analysis

Figure 1 illustrates the methodology employed in this research work. Research has been initiated to study the effect of cavity geometry on base pressure. The geometry is created as a computational nozzle, duct, and cavity model using the ANSYS DesignModeler modeling tool. The cavity geometry includes variations in length-to-depth (L/D) ratios. A computational mesh (grid) is generated for the model. Mesh quality is crucial for correct simulation results. The mesh is refined and checked to ensure that further improvement doesn't notably change the results. The simulation results are validated against specified cases in the literature, with a Cavity Aspect Ratio of 1, L/D Ratios of 2, 4, 6, 8, and 10, and a Nozzle Pressure Ratio (NPR) of 2.65. The percentage difference is less than 10% between simulated and reference results.

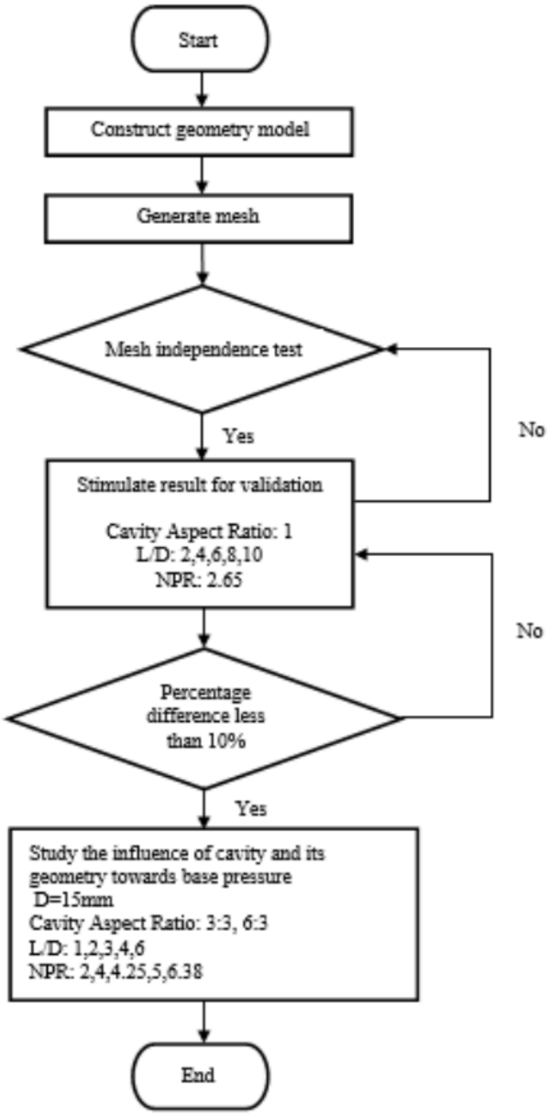

Fig. 1. Methodology flow chart

2.1 CD Nozzle and Enlarged Duct

Figure 2 shows the converging-diverging nozzle with an enlarged duct. The converging-diverging (CD) nozzle plays a vital role in accelerating compressible flows to supersonic speeds and is widely employed in propulsion systems for rockets and jet engines. It comprises three distinct segments: a converging section, a throat (with the smallest cross-sectional area), and a diverging section. Depending on the nozzle's specific geometry and the pressure ratios at the inlet and outlet, the flow exiting the nozzle can be either subsonic or supersonic. In this simulation instance, we will examine the compressible flow within a two-dimensional axisymmetric converging-diverging (CD) nozzle and analyse the flow characteristics under two different operational scenarios.

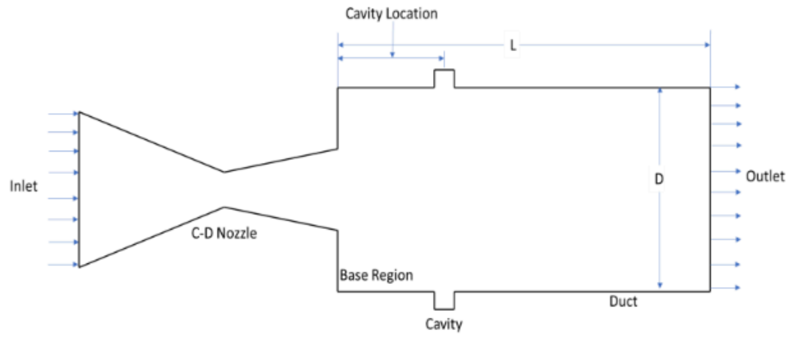

(a) Geometry and nomenclature

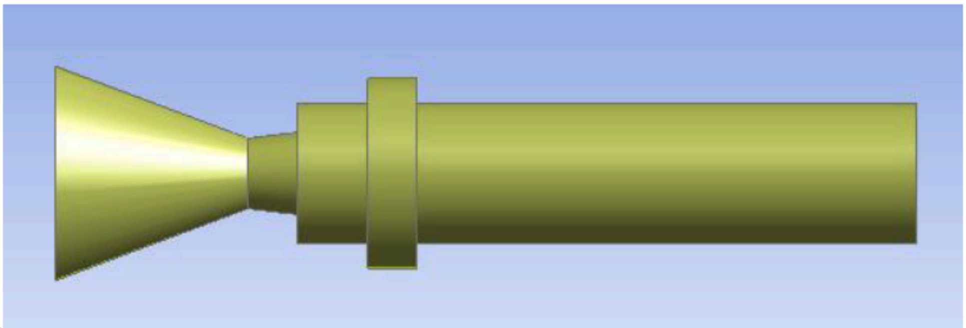

(b) 3D model

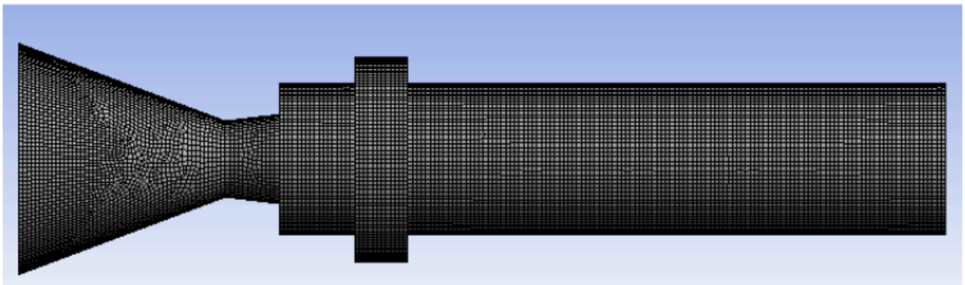

(c) Meshed model

Fig. 2. A convergent-divergent nozzle with a duct and annular cavities

Table 1 shows the parameters and the dimensions of the geometry considered for the analysis. The dimensions of the nozzle are calculated for a Mach number of 1.6. The geometry and 3D model are created based on the dimensions present in Table 1. The area ratio, i.e., the duct cross-sectional area to the nozzle exit area, is considered to be 2.25, and the duct diameter is calculated to be 15 mm.

Table 1
Parameters of the present work

Parameter	Dimension
Convergent angle	20°
Divergent angle	5°
Inlet diameter	25.9 mm
Outlet diameter	10 mm
Throat diameter	8.94 mm
Convergent length	23.3 mm
Divergent length	6.06 mm
Duct diameter	15 mm
Duct length	Depends on the L/D ratio

2.2 Cavity Dimensions and Locations

The aspect ratios for the cavity are considered to be 3:3 and 6:3. Table 2 shows the cavity dimensions according to these aspect ratios.

Table 2
The cavity dimension based on the aspect ratio

Cavity Aspect Ratio, AR	Width (mm)	Height (mm
1	3	3
2	6	3

The placement locations for the cavity, relative to the duct diameter, from the base region are shown in Table 3.

Table 3
The cavity location from the base pressure wall

Cavity Aspect Ratio, AR	Distance from the base pressure, mm	
	AR 1 (3:3)	AR 2 (3:6)
0.5D	6	4.5
1D	13.5	12
1.5D	21	19.5
2D	28.5	27

2.3 Nozzle Pressure Ratio (NPR)

According to the Gas Tables, the NPR for the correct expansion for Mach 1.6 is 4.25. The model's design condition served as the established value. In instances of overexpansion, the chosen values (2, 4) were less than the design condition, while for under-expanded scenarios, the selected values (5, 6.38) surpassed the design condition.

2.4 Grid Independence Test

The grid independence test is crucial for determining the optimal mesh element size. The test was conducted, and the results are presented in Table 4. Based on the results, the element size of 1 mm is considered for further analysis.

Table 4
Grid independence test: Number of mesh elements with various element sizes

Mesh Element size in mm	No. of Element	Base Pressure
5	1304	0.610057
4	1264	0.635878
3	1440	0.612463
2	2796	0.477677
1	15768	0.33163
0.5	111300	0.331748
0.25	885038	0.331865
0.1	13174410	0.331983

3. Results and Discussions

Before analysing the data, it would be enlightening to comprehend the underlying physics of the abruptly increased flow field. In the case of subsonic flows, the boundary layer near the nozzle exit expands as a free shear layer. Eventually, it comes into contact with the immense duct wall downstream, as illustrated in Figure 3. The location where the flow becomes reattached is referred to as the reattachment point. The reattachment length refers to the distance between the base and the reattachment point. The area bounded by the outer edge of the free shear layer, the base, and the point where reattachment occurs will contain one or more vortices. The first vortex, located near the base and quite strong in intensity, is called the primary vortex. This device is a pump transferring fluid from the base to the primary flow on the opposite side of the free shear layer boundary. As a result of this pumping mechanism, there is a decrease in pressure at the base. However, due to the periodic nature of vortex shedding, the pumping follows a regular pattern. Consequently, the base pressure also varies.

Nevertheless, the fluctuations in the pressure were generally found to be minimal and can be expressed as an average value. The nature of the vortex motion leads to the entire flow field in the duct exhibiting periodic behaviour. The oscillations may escalate to a severe level when a combination of specific flow and geometrical characteristics is present. The magnitude of suction at the base and the fluctuations in flow within the duct are heavily influenced by the reattachment and the flow Mach number, which govern the intensity of the primary vortex. At supersonic Mach values, the nozzle outlet will exhibit either an oblique shock ring or an expansion fan ring, depending on whether the flow is overexpanded or underexpanded. During expansion, the flow undergoes acceleration and diverges. The increased rotation, combined with the rotation caused by unrestricted expansion, will result in premature reattachment and a reduced reattachment length.

Regarding oblique shock, it causes the flow to redirect towards the midline of the duct, thereby prolonging the reattachment process and resulting in an increased reattachment length. Therefore, in both scenarios, as the base pressure and flow field oscillations are contingent on the primary vortex, the intensity of the waves will be significantly affected. Annular grooves in the duct will generate extra vortices shed at the hollow. These smaller vortices will function as agents that enhance mixing, potentially increasing the base pressure.

In this study, base flow is controlled through passive means through the cavity. The Mach number of the present study is M = 1.6, and the duct diameter is 15 mm, resulting in an area ratio of 2.25. isentropic relations, the NPR for Mach 1.6 is 4.25. The model's design condition served as the established value. In instances of overexpansion, the chosen values (2, 4) were less than the design NPRs. In contrast, for under-expanded scenarios, the selected values are 5 and 6.38, which are 18% and 50% higher than the required values for correct expansion.

The results of the literature verify the CFD analysis. Pandey *et al. [31] experimentally studied the effect of a cavity on base pressure, and the present results are validated against their*s. Figure 3 shows that the CFD analysis results agree with the experimental results.

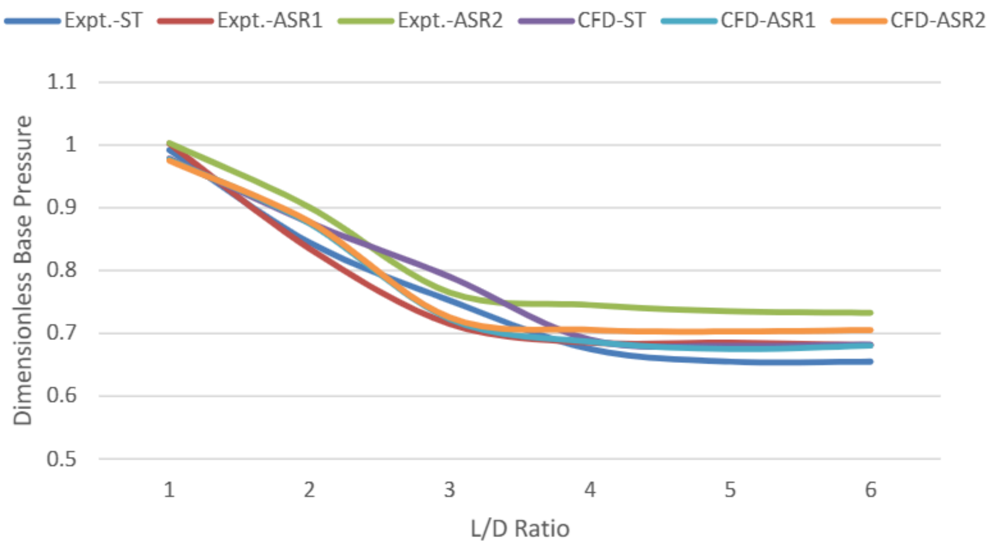

Fig. 3. Validation of CFD analysis results with experimental results [41]

3.1 Influence of Cavity and Its Geometry on Base Pressure at 0.5D location

Base pressure results for both cavities at the 0.5 D location are shown in Figure 4 for various NPRs. Results show that the cavity is ineffective at this location, as the reattachment point appears to be beyond this. These results further demonstrate that cavities have a marginal effect on higher L/D Ratios. This marginal effect may be due to the influence of the significant duct length, where ambient pressure has a minimal impact compared to the small duct lengths, namely L/D = 1, 2, and 3. These results show that the cavity with a larger width is comparatively more effective than the cavity with a width of 3 mm and an aspect ratio of 1. It is also observed that with a decrease in over-expansion level, the efficacy of passive control improves and is at its best when the nozzles are flowing under the influence of a favourable pressure gradient. Therefore, these results reiterate that the control efficiency is optimal whenever the nozzle operates under a favourable pressure gradient.

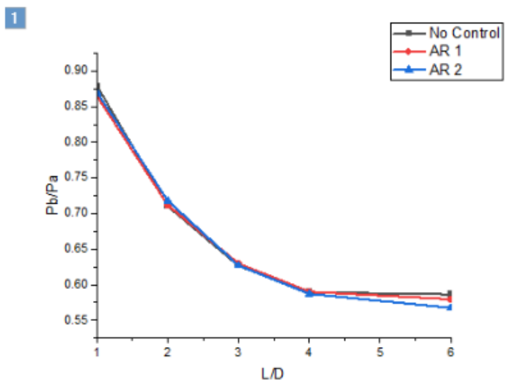

(a) NPR 2 for 0.5D

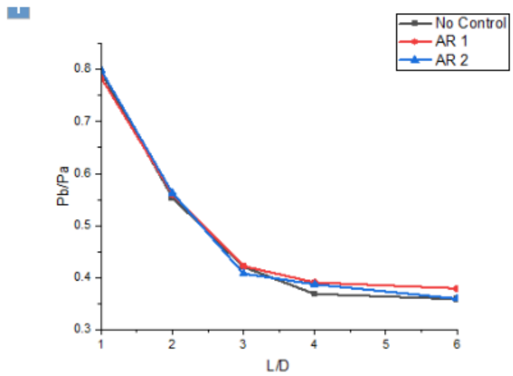

(b) NPR 4 for 0.5D

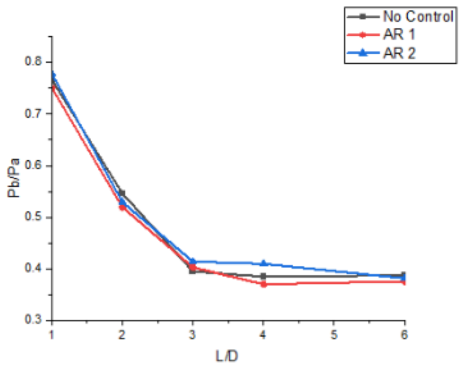

(c) NPR 4.25 at 0.5D

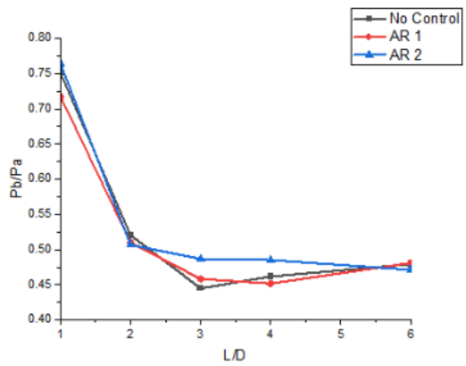

(d) NPR 5 at 0.5D

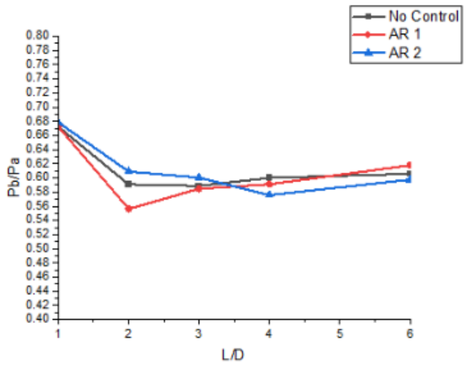

(e) NPR 6.38 at 0.5D

Fig. 4. The base pressure ratio Vs. L/D for plain duct and duct with control with different aspect ratios when a cavity is placed at 0.5D

3.2 Influence of Cavity and Its Geometry on Base Pressure at 1D Location

Base pressure results for both cavities at the 1D location are shown in Figure 5 for various NPRs. Results show that the cavity is effective at this location as the reattachment point seems to be near this location. It is found that when jets are over-expanded, the flow while exiting the nozzle will be accompanied by an oblique shock wave, resulting in higher base pressure values at NPR = 2. It is also observed that at lower L/D Ratios, namely L/D = 1, 2, and 3, the base pressure assumes higher values. This increase in base pressure is attributed to the influence of atmospheric pressure within the duct flow field. There is also a progressive decrease in the base pressure, and flow stabilizes from L/D = 3 and above. It does not exhibit a definite trend and therefore needs to be analyzed on a case-by-case basis. Another reason could be that the reattachment location is influenced by the L/D ratio (i.e., the duct size), the level of expansion, and the aspect ratio of the cavities.

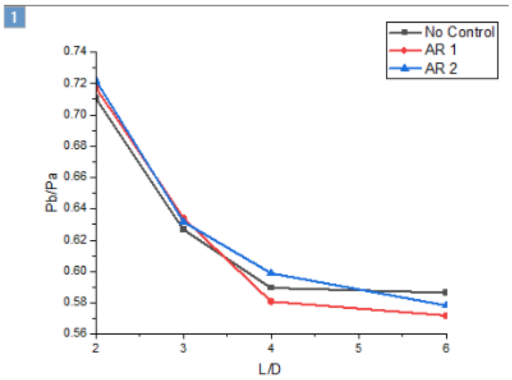

(a) NPR 2 for 1D

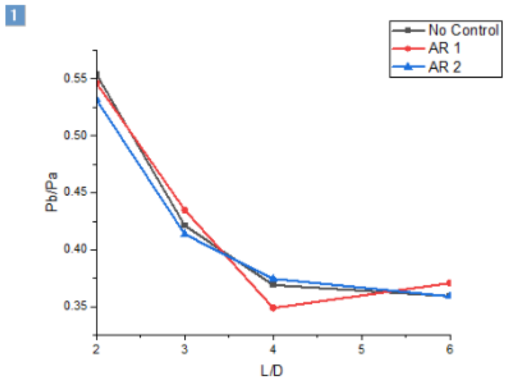

(b) NPR 4 for 1D

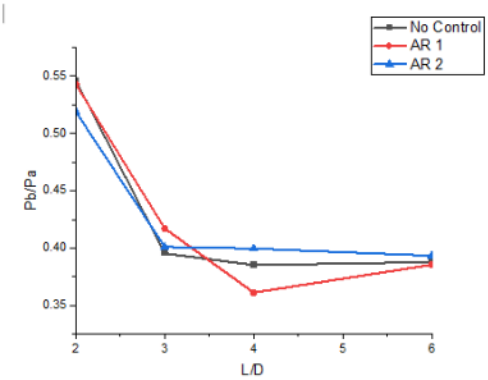

(c) NPR 4.25 at 1D

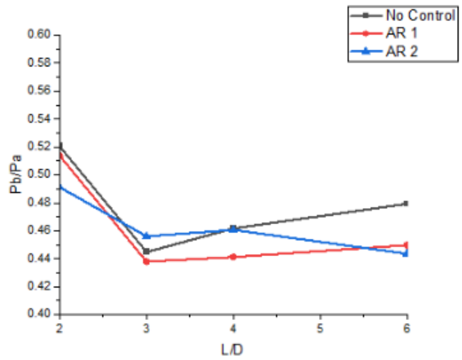

(d) NPR 5 at 1D

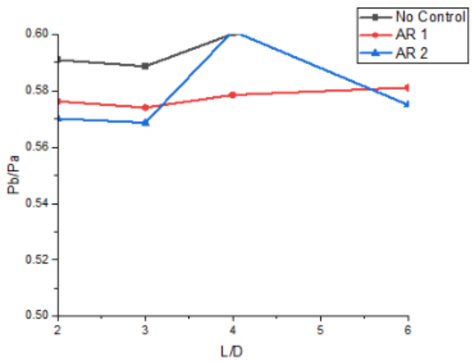

(e) NPR 6.38 at 1D

Fig. 5. The base pressure ratio Vs. L/D for plain duct and duct with control with different aspect ratios when a cavity is placed at 1D

3.3 Influence of Cavity and Its Geometry on Base Pressure at 1.5D Location

Base pressure results for both cavities at 1.5D locations are shown in Figure 6 for various NPRs. The decreasing trend in the base pressure is seen as the nozzle is over-expanded. However, with the progressive increase in base pressure, there is a decrease in the level of over-expansion, and this decreasing trend in base pressure continues until the nozzle is correctly expanded or under-expanded. Results show that the cavity is effective at this location, as the reattachment point appears to be near this location.

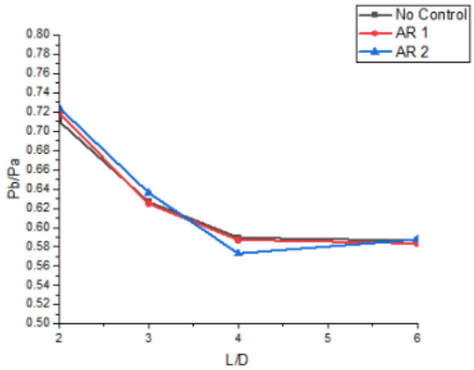

(a) NPR 2 for 1.5D

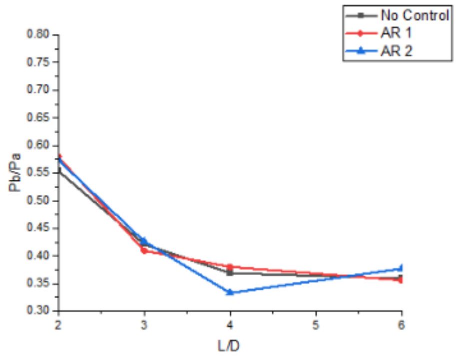

(b) NPR 4 for 1.5D

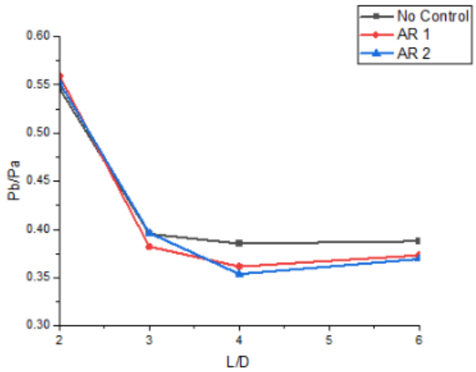

(c) NPR 4.25 at 1.5D

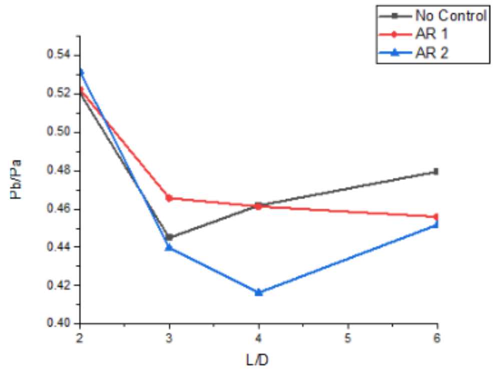

(d) NPR 5 at 1.5D

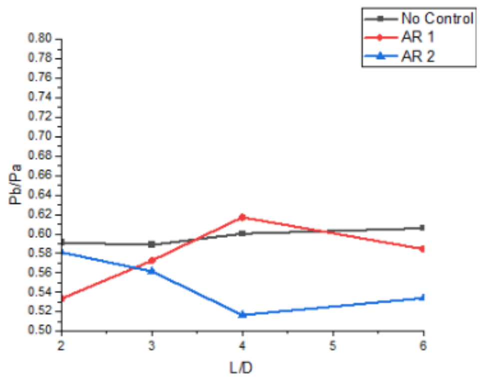

(e) NPR 6.38 at 1.5D

Fig. 6. The base pressure ratio Vs. L/D for plain duct and duct with control with different aspect ratios when a cavity is placed at 1.5D

3.4 Influence of Cavity and Its Geometry on Base Pressure at 2D location

Figure 7 shows the base pressure results for both cavities at the 2D location for various NPRs. The results indicate that the cavity is effective at this location, as the reattachment point appears to be near this location.

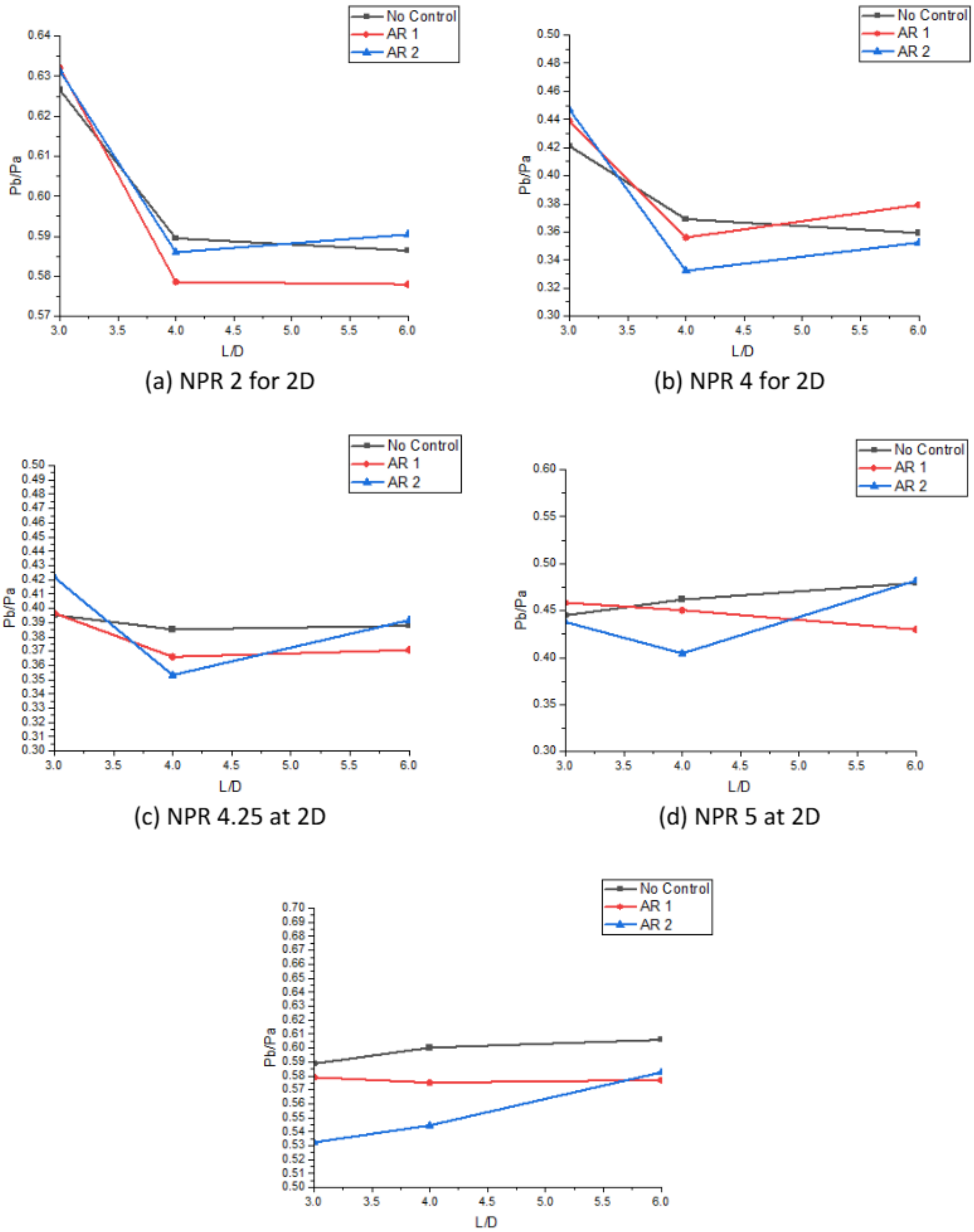

(a) NPR 2 for 2D

(b) NPR 4 for 2D

(c) NPR 4.25 at 2D

(d) NPR 5 at 2D

(e) NPR 6.38 at 2D

Fig. 7. The base pressure ratio Vs. L/D for plain duct and duct with control with different aspect ratios when a cavity is placed at 2D

3.5 Influence of Cavity and Its Geometry on Base Pressure for Various NPRs at 0.5D

Figure 8 shows base pressure results for the cavity with aspect ratios (AR) 3:3 and 6:3 at the 0.5D location for various NPRs at a constant L/D ratio. The results indicate that the cavity is marginally effective at this location (0.5D), as the reattachment point appears to be beyond this location.

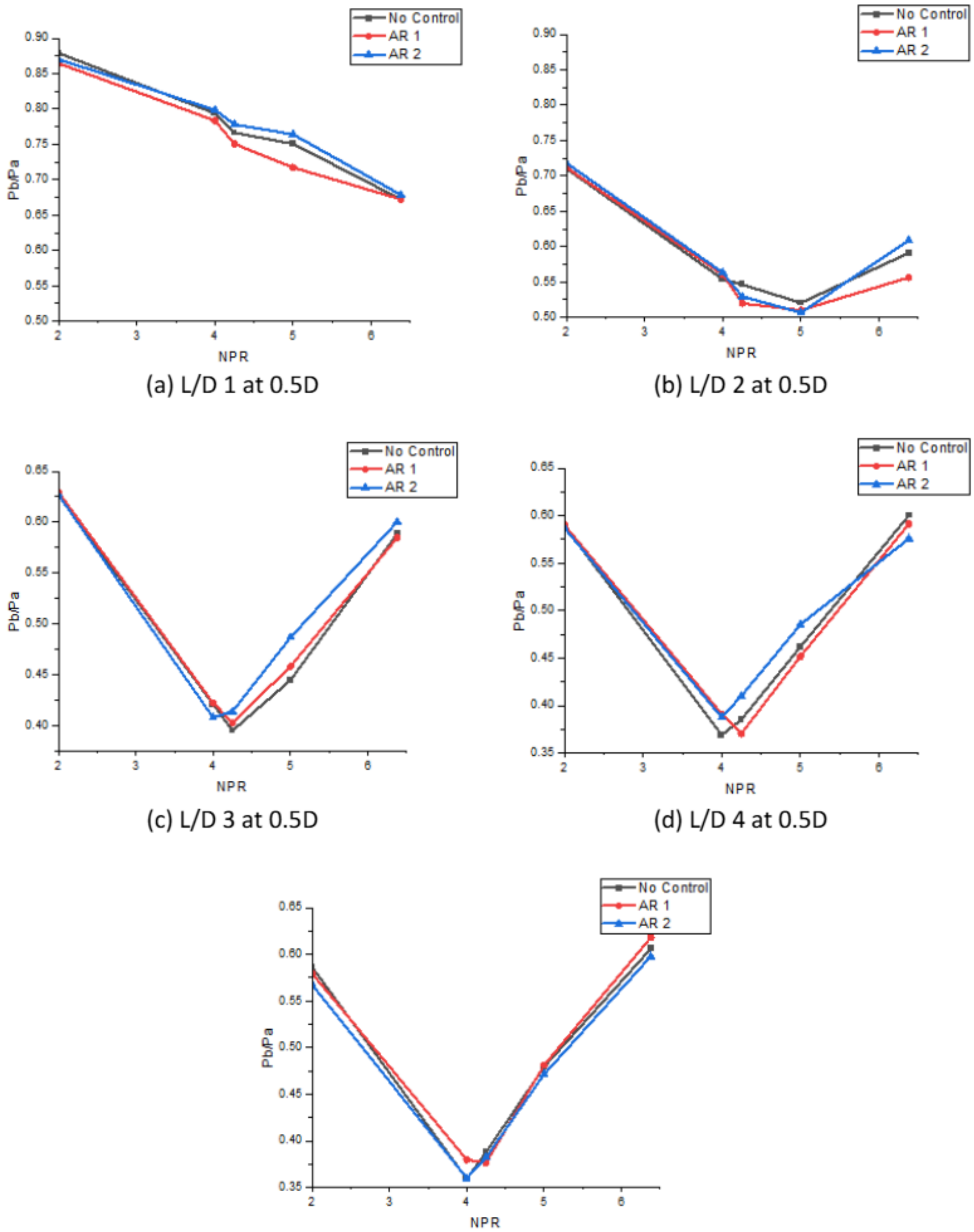

(a) L/D 1 at 0.5D

(b) L/D 2 at 0.5D

(c) L/D 3 at 0.5D

(d) L/D 4 at 0.5D

(e) L/D 6 at 0.5D

Fig. 8. The base pressure ratio vs. NPR with control of different duct lengths for the cavity located at 0.5D

3.6 Influence of Cavity and Its Geometry on Base Pressure for Various NPRs at 1D

Figure 9 shows base pressure results for the cavity with aspect ratios (AR) 3:3 and 6:3 at the 1D location for various NPRs at a constant L/D ratio. The results indicate that the cavity is effective at this location (1D), as the reattachment point appears to be near this location.

CFD Letters
Volume 18, Issue 2 (2026) 103-123

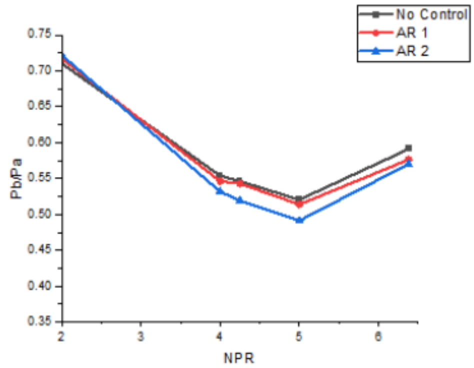

(a) L/D 2 at 1D

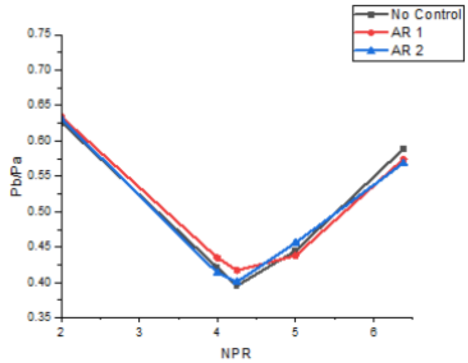

(b) L/D 3 at 1D

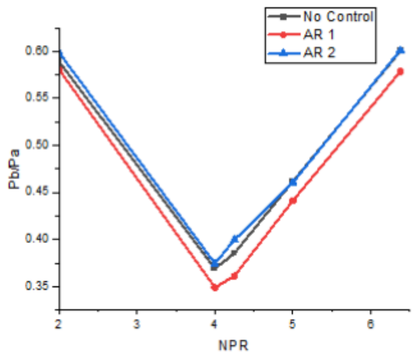

(c) L/D 4 at 1D

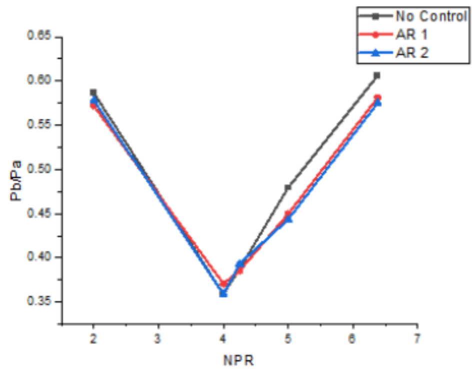

(d) L/D 6 at 1D

Fig. 9. The base pressure ratio variations with NPR with and without control with different duct lengths for a Cavity location at 1D

3.7 Influence of Cavity and Its Geometry on Base Pressure for Various NPRs at 1.5D

Figure 10 shows the base pressure results for the cavity with aspect ratios (AR) 3:3 and 6:3 at the 1.5D location for various NPRs at a constant L/D ratio. The results indicate that the cavity is effective at this location (1.5D), as the reattachment point appears to be near this location.

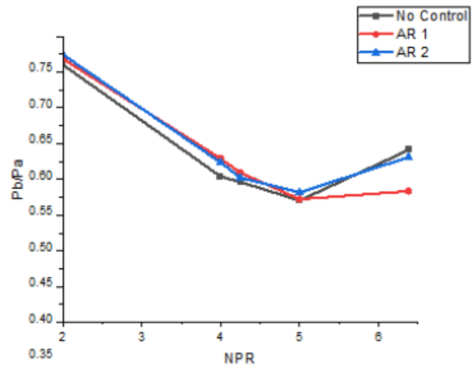

(a) L/D 2 at 1.5D

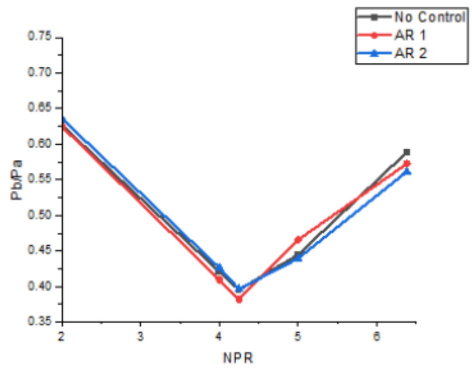

(b) L/D 3 at 1.5D

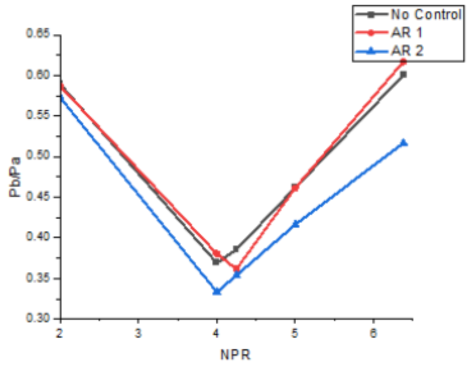

(c) L/D 4 at 1.5D

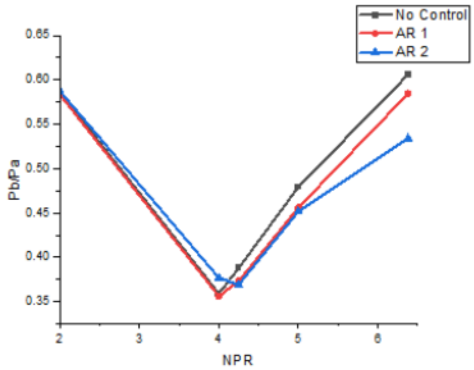

(d) L/D 6 at 1.5D

Fig. 10. The base pressure ratio variations with NPR with and without control with different duct lengths for a Cavity location at 1.5D

3.8 Influence of Cavity and Its Geometry on Base Pressure for various NPRs at 2D

Figure 11 shows base pressure results for the cavity with aspect ratios (AR) 3:3 and 6:3 at a 2D location for various NPRs at a constant L/D ratio. The results indicate that the cavity is effective at this location (2D), as the reattachment point appears to be near this location.

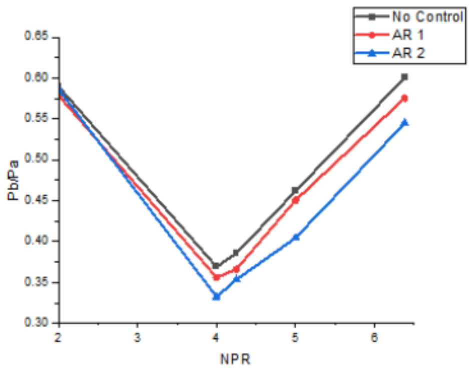

(a) L/D 3 at 2D

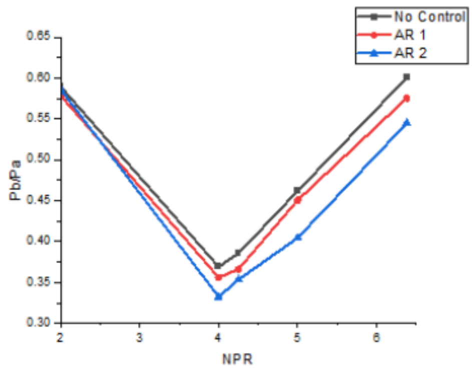

(b) L/D 4 at 2D

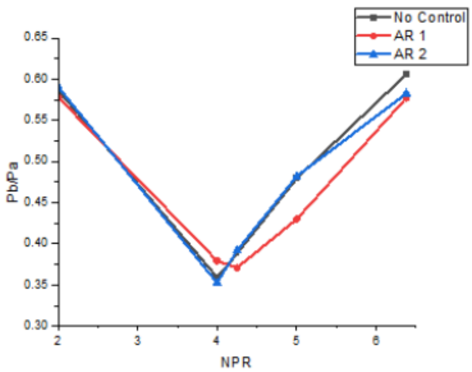

(c) L/D 6 at 2D

Fig. 11. The base pressure ratio variations with NPR with and without control with different duct lengths for a Cavity location at 2D

3.9 Static Pressure Contours

Figure 12 shows the static pressure contours, the variation of pressure fields in the suddenly expanded supersonic flow for Mach 1.74, area ratio 2.89, and NPR 2.65. These contours can help visualize the flow behaviour, recirculation zones, and shock structures resulting from the sudden expansion. Based on the contours, it can be seen that in the immediate downstream region after sudden expansion, the contours show lower pressure zones, highlighting the recirculatory flow where the base pressure drops notably. The pressure contours develop as the L/D ratio increases from 2 to 10. The flow hasn't fully developed at lower L/D, i.e., two orders, and the cavity's influence on base pressure control is not maximized. At moderate L/D, i.e., 6, optimal interaction is observed where the cavity effectively influences the flow field, indicating efficient passive control. At higher L/D ratios, i.e., 8 or 10, the flow appears to reattach before reaching the cavity region, thereby reducing the effectiveness of the control. The contours also depict a gradual pressure rise downstream as the flow stabilizes and reattaches, indicating the end of the recirculation zone and the re-establishment of streamlined flow.

The alternating high and low-pressure zones downstream of the nozzle exit can also be observed in the pressure contour plots. These are indicative of diamond shocks. The diamond shocks are a cycle of compression and expansion waves created due to variations between the exit pressure of the nozzle and the ambient pressure. At lower L/D, i.e., 2 and 4, the diamond shock pattern is more prominent and closer to the nozzle exit. That suggests the shock cell structures have more room to develop due to a shorter duct length. These visible bands of high and low pressure indicate a mismatch of pressures and demonstrate a strong interaction with the base flow recirculation region.

At higher L/D, i.e., 6, 8, 10, the pattern becomes less distinct or is pushed further downstream. That indicates flow stabilization or reattachment and a weaker shock structure within the duct.

The presence of diamond shocks highlights the jet's supersonic nature and the need for effective base pressure regulation. These structures interact with recirculation zones, and well-designed cavities can break or weaken these shock patterns, reducing pressure fluctuations and base drag. Their disappearance or weakening at optimized cavity placements can support the idea that passive control smooths out the flow.

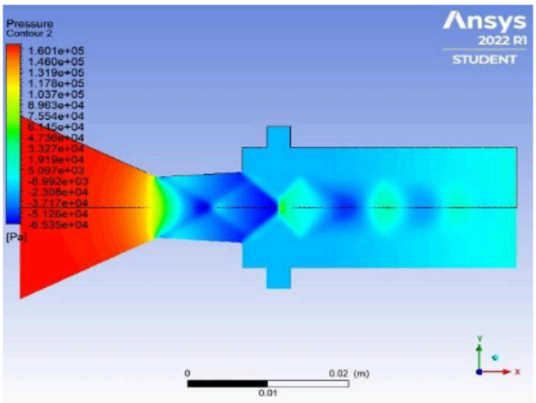

(a) L/D = 2

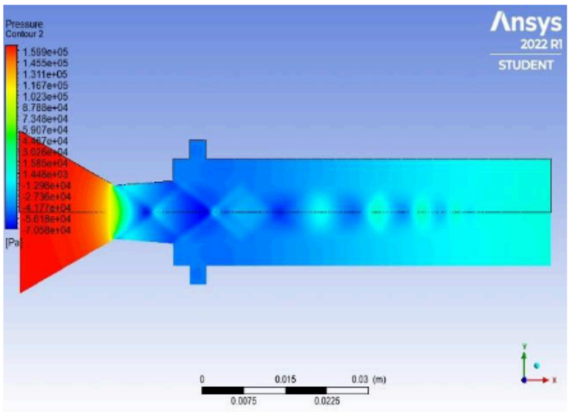

(b) L/D = 4

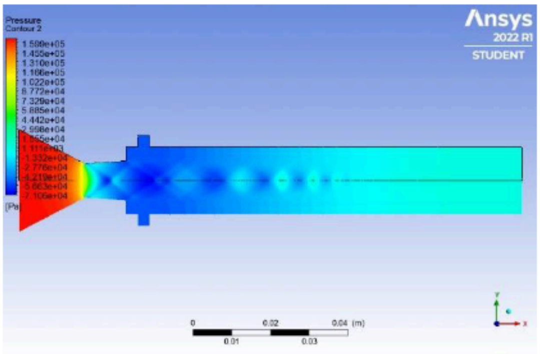

(c) L/D = 6

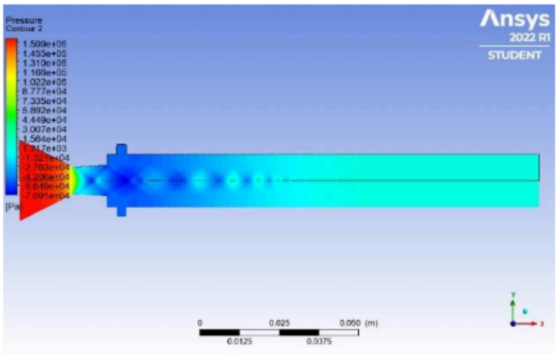

(d) L/D = 8

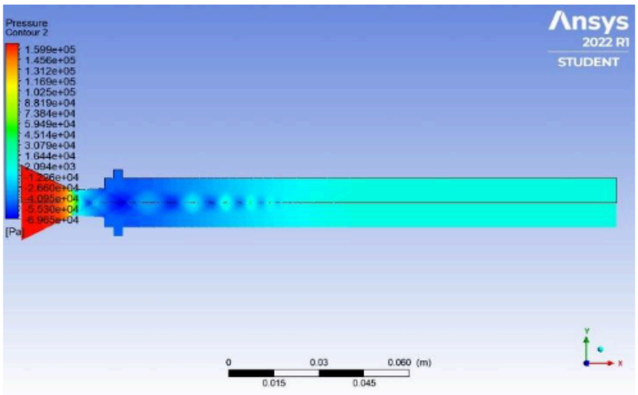

(e) L/D = 10

Fig. 12. Static pressure contour at Mach number 1.74, area ratio 2.89, and NPR 2.65

3.10 Contours, Streamlines and Velocity Vectors for Mach No. 1.6, NPR = 6, L/D = 5, and cavity location = 0.5D

Figures 13 to 17 show the pressure contour, velocity contour, turbulence intensity, streamlines, and velocity vectors in the suddenly expanded supersonic flow for Mach 1.6, NPR = 6, L/D = 5, and cavity location = 0.5D. These contours can help to visualize the flow behaviour and the recirculation zones resulting from the sudden expansion. Figures 13 to 17 show that the contours in the immediate downstream region after a sudden expansion exhibit lower pressure zones, highlighting the recirculatory flow where the base pressure drops notably. The interaction of the cavity with the flow field is observed, where the cavity effectively influences the flow field, indicating efficient passive control. The contours also depict a gradual pressure rise downstream as the flow stabilizes and reattaches, signifying the end of the recirculation zone and the re-establishment of streamlined flow.

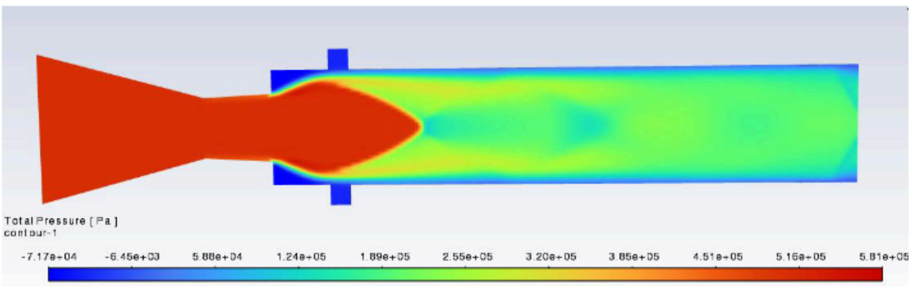

Fig. 13. Total pressure contour: Mach 1.6, NPR = 6, L/D = 5, Location = 0.5D

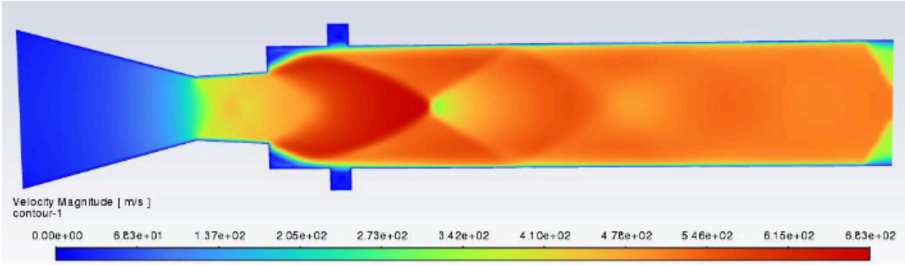

Fig. 14. Velocity contour: Mach 1.6, NPR = 6, L/D = 5, Location = 0.5D

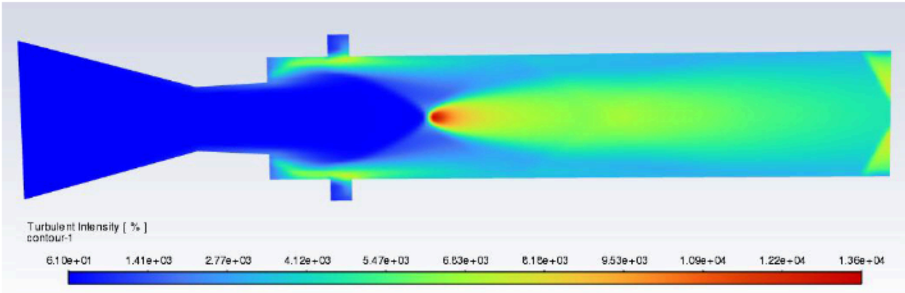

Fig. 15. Turbulence intensity contour: Mach 1.6, NPR = 6, L/D = 5, Location = 0.5D

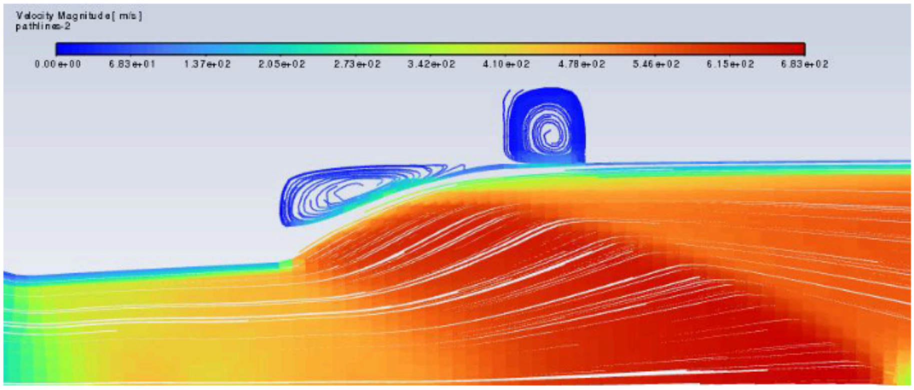

Fig. 16. Streamlines near base region coloured by velocity: Mach 1.6, NPR = 6, L/D = 5, Location = 0.5D

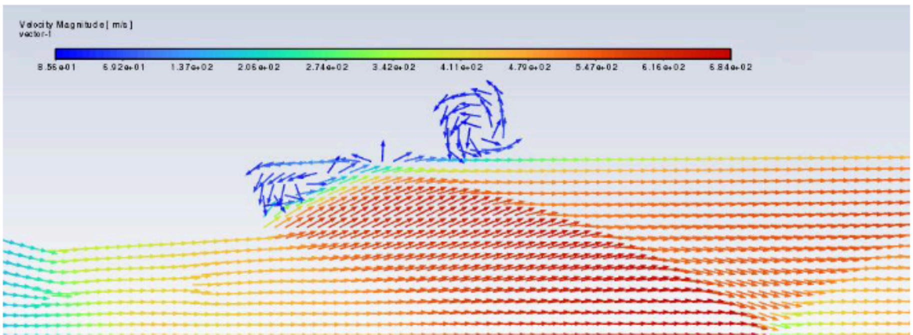

Fig. 17. Velocity vectors near base region: Mach 1.6, NPR = 6, L/D = 5, Location = 0.5D

4. Conclusion

In summary, the base pressure is influenced by several factors, including the level of expansion, Mach number, area ratio (L/D ratio), cavity dimensions, and cavity location. The effectiveness of passive control is contingent upon the cavity's location, with ineffectiveness noted beyond the reattachment point. The literature review suggests that active and passive control measures prove effective when jets experience a favourable pressure gradient, while their efficacy diminishes in over-expanded jet conditions. Interestingly, the depth of the cavity does not significantly impact its effectiveness compared to its length. Furthermore, passive control is most effective when the dividing streamline falls within the cavity's length.

5. Scope for Future Work

Several avenues merit exploration to enhance our understanding of base pressure control and optimize aerodynamic performance in high-speed flows. Further research could explore the development and application of innovative passive control strategies, taking into account emerging technologies and materials. Exploring the influence of real-world conditions, such as turbulence and external disturbances, on the efficacy of passive control methods would also be beneficial.

Furthermore, investigating the application of machine learning algorithms to predict and optimize base pressure under diverse scenarios could open new avenues for efficient aerodynamic design. Collaborative efforts among researchers in fluid dynamics, materials science, and control systems engineering could lead to holistic solutions for base pressure management in high-speed aerodynamic flows.

Acknowledgement
This research was not funded by any grant.

References
[1] Rathakrishnan, E. 2001. "Effect of Ribs on Suddenly Expanded Flows." AIAA Journal 39 (7): 1402–1404.
[2] Rathakrishnan, E. 1999. "Effect of Splitter Plate on Bluff Body Drag." AIAA Journal 37 (9): 1125–1126. https://doi.org/10.2514/2.823.
[3] Baig, M. A. A., S. A. Khan, Al-Mufadi, Fahad, and E. Rathakrishnan. 2011. "Control of Base Flows with Microjets." International Journal of Turbo Jet Engines 28 (1): 59–69. https://doi.org/10.1515/TJJ.2011.009.
[4] Rathakrishnan, E. 2015. "Base Pressure Control by Using Ribs in Subsonic and Sonic Suddenly Expanded Flows." AIAA Conference Proceedings.
[5] Vijayaraja, K., C. Senthilkumar, S. Elangovan, and E. Rathakrishnan. 2014. "Base Pressure Control with Annular Ribs." International Journal of Turbo Jet Engines 31 (2): 111–118. https://doi.org/10.1515/tjj-2013-0037.
[6] Sethuraman, V., P. Rajendran, S. A. Khan, A. Aabid, and M. Baig. 2024. "Control of Nozzle Flow Using Rectangular Ribs at Sonic and Supersonic Mach Numbers." Fluid Dynamics and Materials Processing. https://doi.org/10.32604/fdmp.2024.049441.
[7] Sethuraman, V., P. Rajendran, and S. A. Khan. 2020. "Base and Wall Pressure Control Using Cavities and Ribs in Suddenly Expanded Flows – An Overview." Journal of Advanced Research in Fluid Mechanics and Thermal Science 66 (1): 120–134.
[8] Khan, A., S. A. Khan, V. Raja, A. Aabid, and M. Baig. 2024. "Effect of Ribs in a Suddenly Expanded Flow at Sonic Mach Number." Heliyon 10 (9): e30313. https://doi.org/10.1016/j.heliyon.2024.e30313.
[9] Khan, A., A. Aabid, M. N. Akhtar, S. A. Khan, and M. Baig. 2025. "Supersonic Flow Control with Quarter Rib in a Duct: An Extensive CFD Study." International Journal of Thermofluids 26: 101060. https://doi.org/10.1016/j.ijft.2025.101060.
[10] Azami, M. H., M. Faheem, A. Aabid, I. Mokashi, and S. A. Khan. 2019. "Inspection of Supersonic Flows in a CD Nozzle Using an Experimental Method." International Journal of Recent Technology and Engineering 8 (2S3): 996–999.
[11] Pathan, K. A., P. S. Dabeer, and S. A. Khan. 2020. "Enlarge Duct Length Optimization for Suddenly Expanded Flows." Advances in Aircraft and Spacecraft Science 7 (3): 203–214.
[12] Khan, A., A. Aabid, S. A. Khan, M. N. Akhtar, and M. Baig. 2024. "Comprehensive CFD Analysis of Base Pressure Control Using Quarter Ribs in Sudden Expansion Duct at Sonic Mach Numbers." International Journal of Thermofluids 24 (October): 100908. https://doi.org/10.1016/j.ijft.2024.100908.

[13] Khan, A., S. A. Khan, M. N. Akhtar, A. Aabid, and M. Baig. 2024. "Base Pressure Control with Semi-Circular Ribs at Critical Mach Number." Fluid Dynamics and Materials Processing 22. https://doi.org/10.32604/fdmp.2024.049368.
[14] Khan, A., N. M. Mazlan, and E. Sulaeman. 2022. "Effect of Ribs as Passive Control on Base Pressure at Sonic Mach Numbers." CFD Letters 14 (1): 140–151. https://doi.org/10.37934/cfdl.14.1.140151.
[15] Hai-bo, and W.-q. Liu. 2012. "Influence of Cavity Length on Forward-Facing Cavity and Opposing Jet Combined Thermal Protection System Cooling Efficiency." International Journal of Aerospace and Mechanical Engineering.
[16] Heubner, L. D., and L. J. Utreja. 1993. "Mach 10 Bow Shock Behaviour of Forward-Facing Nose Cavity." Journal of Spacecraft and Rockets 30: 291–297. https://doi.org/10.2514/3.25513.
[17] Lorite, M., et al. 2017. "Drag Reduction of Slender Blunt-Based Bodies Using Optimized Rear Cavities." Journal of Fluids and Structures. https://doi.org/10.1016/j.jfluidstructs.2017.07.011.
[18] Sanmiguel, E., and M.-A. Alcantara. 2014. "Drag Reduction Induced by the Addition of a Multi-Cavity at the Base of a Bluff Body." Journal of Fluids and Structures. https://doi.org/10.1016/j.jfluidstructs.2014.03.013.
[19] Kavimandan, M., and B. Chandrasheker. 2020. "Aerothermodynamic Analysis of a Blunt Body with Forward-Facing Cavity and Opposing Jet Combination." International Journal of Engineering Research and Technology (IJERT).
[20] Saravanan, G., G. Jagadeesh, and K. P. J. Reddy. 2009. "Investigation of the Missile-Shaped Body with Forward-Facing Cavity at Mach 8." Journal of Spacecraft and Rockets 46: 577–591. https://doi.org/10.2514/1.38914.
[21] Sudarshan, S., and S. M. V. Rao. 2021. "Effect of the Axial Cavity with an Opposing High-Pressure Jet Combination in a Mach 6 Flow Condition." Acta Astronautica. https://doi.org/10.1016/j.actaastro.2020.09.021.
[22] Mohandas, S., and B. John. 2019. "Reduction of Wave Drag on Parameterized Blunt Bodies Using Spikes with Varied Tip Geometries." Acta Astronautica. https://doi.org/10.1016/j.actaastro.2019.04.017.
[23] Engblom, W. A., B. Yuceil, D. B. Goldstein, and D. S. Dolling. 1995. "Hypersonic Forward-Facing Cavity Flow: An Experimental and Numerical Study." AIAA Paper 95-0293. https://doi.org/10.2514/6.1995-293.
[24] Huang, W., and Z.-t. Zhao. 2017. "Parametric Study on the Drag and Heat Flux Reduction Mechanism of a Forward-Facing Cavity on a Blunt Body in Supersonic Flows." Aerosp. Science and Technology. https://doi.org/10.1016/j.ast.2017.10.017.
[25] Santos, W. F. N. 2007. "Simulation of Blunt Leading Edge Aerothermodynamics in Rarefied Hypersonic Flow." Journal of the Brazilian Society of Mechanical Sciences and Engineering 29 (2): 39–51. https://doi.org/10.1590/S1678-58782007000200001.
[26] Khan, S. A., Asadullah, M., Fharukh Ahmed, G.M., Jalaluddeen, Ahmed, Ali Baig, Maughal Ahmed. 2018. "Passive Control of Base Drag in Compressible Subsonic Flow Using Multiple Cavities." International Journal of Mechanical and Production Engineering Research and Development 8 (4): 39–4431.
[27] Khan, S. A., Asadullah, M., Sadiq, J. 2018. "Passive Control of Base Drag Employing Dimple in Subsonic Suddenly Expanded Flow." International Journal of Mechanical and Mechatronics Engineering 18 (3): 69–74.
[28] Sajali, M. F. M., Aabid, A., Khan, S. A., Mehaboobali, F. A. G., Sulaeman, E. 2019. "Numerical Investigation of the Flow Field of a Non-Circular Cylinder." CFD Letters 11 (5): 37–49.
[29] Khan, S. A., and E. Rathakrishnan. 2006. "Nozzle Expansion Level Effect on Suddenly Expanded Flow." International Journal of Turbo Jet Engines 23 (4): 233–257
[30] Khan, S. A., and E. Rathakrishnan. 2005. "Active Control of Suddenly Expanded Flow from Under-Expanded Nozzles—Part II." International Journal of Turbo Jet Engines 22 (3): 163–183. https://doi.org/10.1515/TJJ.2005.22.3.163.
[31] K M Pandey and E Rathakrishnan. "Influence of Cavities on Flow Development in Sudden Expansion." International Journal of Turbo and Jet Engines 23, (2006): 97-112. http://dx.doi.org/10.1515/TJJ.2006.23.2.97